ARTICLES

Location of Butanol in Mixed Micelles with Alkyl Glucosides Studied by SANS

A. Möller,* P. Lang, and G. H. Findenegg

Iwan-N.-Stranski-Institut für Physikalische und Theoretische Chemie, Technische Universität Berlin, Strasse des 17. Juni 112, 10623 Berlin, Germany

U. Keiderling

Hahn-Meitner-Institut Berlin, Glienicker Strasse 100, 14109 Berlin, Germany, and Institut für Metallforschung, Technische Universität Berlin, Hardenbergstrasse 36, 10623 Berlin, Germany

Received: April 13, 1998; In Final Form: June 30, 1998

Aqueous micellar solutions of β-D-octyl glucopyranoside (β-C_8G_1), β-D-decyl maltopyranoside (β-$C_{10}G_2$), and β-D-dodecyl maltopyranoside (β-$C_{12}G_2$) containing 5 wt % of butanol have been studied by small angle-neutron scattering using contrast matching techniques in order to determine the location of the alcohol molecules in the micelles. At the chosen alcohol content the micelles of all three surfactants take on prolate ellipsoidal shape. Using deuterated butanol in combination with fully protonated surfactants dissolved in an appropriate mixture of H_2O/D_2O, it was possible to obtain a scattering signal solely due to the alcohol. For all three systems under investigation, it was found that butanol is incorporated into the amphiphile film and is not solubilized into the hydrophobic core of the micelles.

Introduction

Due to their amphiphilicity, surfactants are forced to self-assemble if dissolved in water which leads to a wealth of liquid crystalline mesophases at elevated surfactant contents of the mixture. At small concentrations, the surfactants commonly form isotropic micellar solutions as long as there are no further components present in the solution. However, it was shown that the addition of small amounts of alcohols with intermediate chain length ($4 < n < 10$) can induce the formation of lamellar structures in the dilute regime.[1−6] This formation of lamellar phases is believed to be driven by the lowering of the mean curvature of the interface separating the hydrophobic from the hydrophilic part of the surfactant assemblies.[7] Accordingly, one might expect the micellar shape in a given surfactant + water mixture to change from spherical or near-spherical shape to cylindrical and disklike shape upon the successive addition of alcohol before the solution eventually transforms into a lamellar liquid crystal. Actually such behavior has been observed for so-called alkyl polyglycosides (APG, trade name of the Henkel Corp.),[6] i.e., surfactants containing saccharide residues as their hydrophilic moiety. These compounds which are nowadays widely used in commercial products, represent a complex mixture of homologous alkyl glucosides (C_nG_m) with different hydrocarbon chain length and different numbers of glucose units. Also in aqueous solutions of alkyl glucosides with uniform chain length of the hydrophilic and the hydrophobic part like β-octyl glucopyranoside (β-C_8G_1), β-decyl maltopyranoside (β-$C_{10}G_2$), and dodecyl maltopyranoside (β-$C_{12}G_2$), the micellar shape changes upon the addition of alcohol.[8,9] In a preceding study,[8] we have shown that upon addition of 5 wt % of butanol to a 5 wt % aqueous micellar solution of β-C_8G_1, the micelles transform from almost spherical to prolate ellipsoids of revolution with an axial ratio of ca. 10 for the hydrocarbon core. Furthermore, the length of the major semiaxis (i.e., the cross-sectional radius) was found to be independent of the alcohol concentration and to be set by the length of the surfactant molecule. Subsequent studies on the influence of butanol on size and shape of β-$C_{10}G_2$ and β-$C_{12}G_2$ revealed a similar pattern. Both surfactants exhibit a change in the micellar structure from near-spherical to prolate upon the addition of butanol and the characteristic dimension of the micelles; i.e., the cross-sectional radius is again set by the length of the surfactant molecules. As the butanol concentration is further increased, it appears that the micelles start to grow in the second dimension toward an oblate shape. These results will be presented in detail in a forthcoming paper.[9]

In the present contribution we address the question in which way the butanol is incorporated into the micelles of the three C_nG_m surfactants. The experiments were focused to alcohol concentrations at which the micelles of all three surfactants are of prolate shape. It is accepted that short-chain alcohols (up to three carbon atoms), which are miscible with water in all proportions, are adsorbed to the hydrophilic shell of the micelles. On the other hand, water-insoluble medium- and long-chain alcohols (more than four carbon atoms) are solubilized in the hydrophobic core.[10−15] Butanol is intermediate between these two types of solubility behavior and therefore might be incorporated into the micelles in either of the two ways. The location of the alcohol can be determined unambiguously by small-angle neutron scattering (SANS) using contrast variation techniques to separate the scattering of the alcohol from the

10.1021/jp981819q CCC: $15.00
Published on Web 10/21/1998

contribution of the surfactant. For neutrons the coherent scattering length of hydrogen and deuterium have opposite signs and thus give rise to very sizable relative variations of the scattered intensity if protonated and deuterated samples of the same species are compared. In the present case, we seek to reduce the number of "visible" components in order to obtain information on the exact location of the alcohol molecules in compound micelles containing C_nG_m and butanol. For this purpose, a H_2O/D_2O mixture has to be found which has the same scattering length density (SLD) as the compound micelles containing protonated butanol. Replacing the alcohol in these mixtures by deuterated butanol enhances the scattering contrast and the resulting scattering curves bear information on the spatial distribution of the alcohol in the micelles.

Experimental Section

Materials. The chemicals used in this study were purchased from the following supplies: β-D-octyl glucopyranoside (>97%, $M_r = 292.4$), β-D-decyl maltopyranoside (>99%, $M_r = 482.6$), and β-D-dodecyl maltopyranoside (>95%, $M_r = 510.6$) from Calbiochem, 1-butanol (>99.5%, $M_r = 74.12$) from Merck, 1-butanol-d_{10} (>99%, $M_r = 84.12$) from Aldrich, and D_2O (>99.9%, $M_r = 20.3$) from Sigma. All substances were used without further purification.

Small-Angle Neutron Scattering (SANS). SANS measurements were performed at the light water cooled and moderated swimming pool type reactor of the Hahn-Meitner-Institut (HMI), Berlin, Germany, at instrument V4 which is located at the curved neutron guide NL 3A.[16] Neutrons were derived from a liquid hydrogen cold source and monochromated by a mechanical velocity selector. The mean de Broglie wavelength was set to $\lambda_0 = 0.60$ nm with a wavelength distribution with a fwhm of $\Delta\lambda/\lambda_0 = 0.1$. The two-dimensional ^{3}He detector with 64 × 64 elements of 10 × 10 mm^2 was positioned at sample-to-detector distances of 2, 4, and 12 m to cover a range of momentum transfer of 0.04 nm^{-1} < q < 3.15 nm^{-1} after radial averaging of the data. Sampling times were chosen such that the statistical error was smaller than 3% in the higher q range. The solutions were prepared by weight in high-purity water from a Milli-Q water purification system (Millipore Waters) equipped with a 0.2 μm dust filter. All samples contained 5 wt % of the surfactant and 5 wt % of alcohol. The so-called match point, i.e., the H_2O/D_2O mixture which produces the minimum scattering intensity if used as solvent, was estimated by measuring the integral scattered intensity at a sample-to-detector distance of 12 m. Quartz cells with a path length of 1 mm were used as sample containers which were inserted into aluminum sample holders. The temperature was set to 25 °C. The primary data were reduced and evaluated in two steps. In the first step, sample cell scattering and background scattering was subtracted from the raw data, and the resulting two-dimensional data array was normalized to H_2O scattering and subsequently radially averaged. This data reduction procedure was performed with the HMI standard software[17] and was independently applied to the samples and to the pure solvent. In the second step the solvent scattering was subtracted from the sample scattering and the resulting excess scattering data $I(q)$ were analyzed by calculating the corresponding pair−distance distribution functions $p(r)$ by indirect Fourier transformation using Glatter's ITP software.[18] In this algorithm, the $p(r)$ function is constructed from the linear combination of B-spline functions the number of which was set to $N = 10$. Seven basic functions were distributed with equal spacings in the range of $0 < r < 3.5$ nm, and three splines were set equidistantly in the range $3.5 < r < D_{max}$, where D_{max} is the maximum length which can be found in the scattering particle. D_{max} was estimated throughout this contribution by iterative optimization with respect to the stability plot and with respect to the goodness of the approximation of the experimental data by the transformed B-splines as described by Müller and Glatter.[19] Based on the results from this model-independent approach, an appropriate particle scattering factor was chosen to fit the experimental data as will be discussed below.

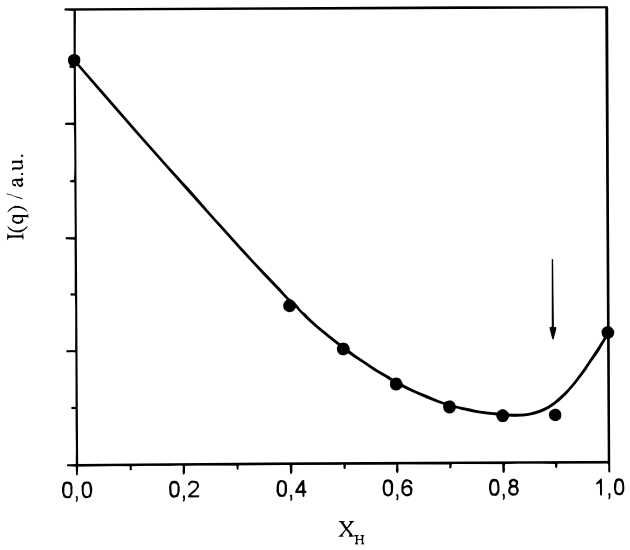

Figure 1. Square root of the scattered intensity $\sqrt{I(q\rightarrow 0)}$ vs the mole fraction of H_2O in the solvent X_H. The arrow indicates the solvent composition used in the contrast matching measurements. The symbols are data from solutions with 5 wt-% surfactant and protonated butanol each, integrated over a range of scattering vectors 0.05 nm^{-1} < q < 0.08 nm^{-1}. The full line is a guide to the eye.

Results and Discussion

Estimation of the Match Point. A series of samples with constant amphiphile ($c_a = 5$ wt %) and butanol content ($c_b = 5$ wt %) but different H_2O/D_2O mixtures ($X_H = 0.0$, 0.6−1.0) as solvent were prepared and the scattering intensities were measured. Since the scattering intensity extrapolated to zero scattering vector $I(q \rightarrow 0)$ can be written as $I(0)^{1/2} = V(\sigma_M - \sigma_S)$, where V is the volume of the micelle, σ_M is the average scattering length density of the micelle, and σ_S the scattering length density of the solvent, the square root of the scattering intensity will show a sharp minimum at the solvent composition representing the SLD of the micelle.[20] This point is called the contrast match point where $\sigma_M = \sigma_S$. If the particles are not uniform in size or shape, or their radial SLD profile is inhomogeneous, there will not be a single solvent composition that matches all micelles or all parts of the micelles. The plot of the square root of the intensity vs solvent composition will exhibit a composition range, where the excess scattering from the micelles is minimal. For convenience, we will further on denote the samples containing protonated butanol as β-C_nG_m-PB and the ones with deuterated butanol accordingly as β-C_nG_m-DB.

In Figure 1 we have plotted the square root of the intensity scattered from solutions containing β-C_8G_1PB vs the molar fraction of H_2O in the solvent mixture X_H. The intensity values represent integrated counts from a range of momentum transfer of 0.05 nm^{-1} < q < 0.08 nm^{-1} (12 m sample−detector distance). As to be expected for solutions of micelles which have radially inhomogeneous scattering length densities, there

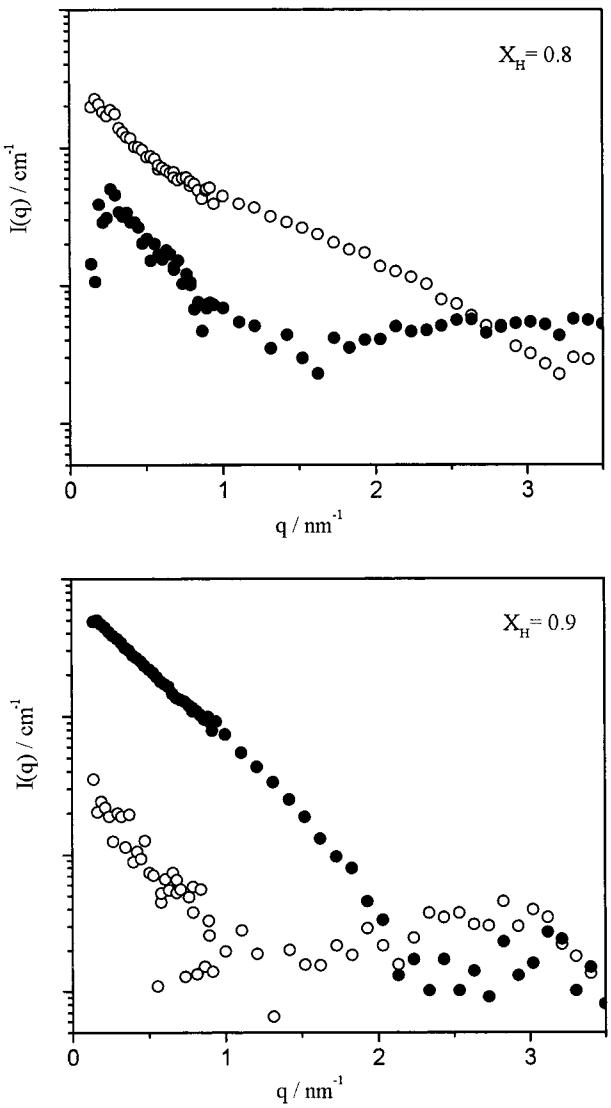

Figure 2. Excess scattering of β-C_8G_1DB (●) and β-C_8G_1PB (○) in solutions with $X_H = 0.8$ (upper) and $X_H = 0.9$ (lower). The intensities are plotted in units of water scattering. In the upper part, the excess scattering from the β-C_8G_1PB sample is even stronger than from the β-C_8G_1DB sample. In the lower part, the excess scattering is enhanced significantly if deuterated butanol is present.

is a plateau of minimum intensity which spans the region of $X_H = 0.8-0.9$. Since β-$C_{10}G_2$ and β-$C_{12}G_2$ are chemically very similar to β-C_8G_1, it is reasonable to assume that the minimum scattering contrast from solutions of these surfactants will occur for solvent mixtures with $X_H \approx 0.8-0.9$ as well. Therefore, we performed scattering experiments with two different solvent compositions, i.e., $X_H = 0.8$ and $X_H = 0.9$ for all three surfactants.

A better estimation of the matchpoint is obtained if the entire scattering curves are considered. Figure 2 shows the radially averaged excess scattering intensities of the solutions containing β-C_8G_1PB and β-C_8G_1DB in both solvent compositions. In the upper part the data from the samples with $X_H = 0.8$ are displayed. As seen in the figure, there is still a significant amount of scattering from the samples with protonated butanol observed. If the alcohol is substituted by deuterated butanol, the excess scattering intensity decreases even further in almost the entire q range. In other words, the mean SLD of the β-C_8G_1-DB micelles is closer to the solvent value than the SLD of the β-C_8G_1PB aggregates. The curves in the lower part of Figure 2 were obtained from samples with $X_H = 0.9$. Here, the β-C_8G_1-

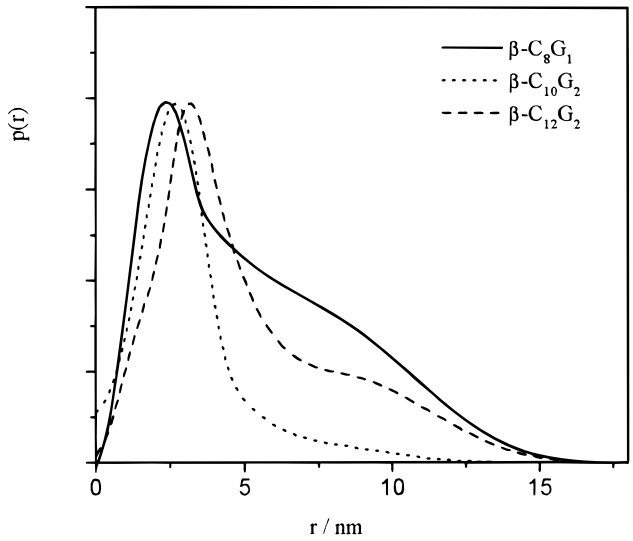

Figure 3. Pair−distance distribution functions $p(r)$ for the samples containing 5 wt % of β-C_8G_1, β-$C_{10}G_2$, and β-$C_{12}G_2$ and 5 wt % of deuterated butanol in a solvent with $X_H = 0.9$. All curves show the typical features expected for elongated particles, i.e., a maximum at rather small distances r and an almost linear decay toward higher r.

PB solution exhibits no significant scattering intensity. If we substitute the protonated butanol by deuterated butanol, the scattering intensities increase by 1 order of magnitude in the low q range. It is thus evident that the solvent with $X_H = 0.9$ has a SLD which matches the compound β-C_8G_1PB micelles better than the mixture with $X_H = 0.8$. The samples containing β-$C_{10}G_2$ and β-$C_{12}G_2$ showed qualitatively the same behavior. We will therefore confine the further discussion to the data from the solutions with $X_H = 0.9$.

Analysis of the Scattering Data. The structural information contained in these scattering curves is almost solely due to the deuterated butanol and therefore allows the determination of the incorporation site of the alcohol. The scattering data from the samples which contain deuterated butanol have been corrected for wavelength smearing and indirectly Fourier transformed using the algorithm developed by Glatter.[18,21] The resulting pair−distance distribution functions p(r) are shown in Figure 3. For all three surfactants they exhibit the typical features of an elongated particle, i.e., a distinct maximum at rather small distances r and an almost linear decay toward higher values of r. In the previous paper,[8] we have shown for β-C_8G_1 that this kind of pair−distance distribution function corresponds to an inhomogeneous prolate ellipsoid of revolution, consisting of a core formed by the hydrophobic alkyl chains with the SLD σ_c and a shell formed by the hydrophilic surfactant headgroups with the SLD σ_s. Concerning the qualitative similarity of the $p(r)$ functions of all three samples, it is likely that the scattering data from the β-$C_{10}G_2$ and β-$C_{12}G_2$ mixtures may be described as well by the particle scattering factor for the core−shell model of an ellipsoid of revolution. This simple qualitative data analysis is based on two assumptions: (i) the particle interaction will not cause any contribution to the scattering curve by interparticle interference, i.e., the solution structure factor $S(q)$ is close to unity in the q range observed, and (ii) the particles are of equal size and shape, i.e., they are monodisperse. This assumptions are justified by the following experimental findings. As we experienced in LS measurements from aqueous solutions of C_8G_1, there is an attractive interaction which effects the scattering data at $q \rightarrow 0$.[8] However, in the q range of SAXS and SANS experiments, the scattered intensity increases linearly with the surfactant weight fraction at any constant q, which

means that $S(q) \approx 1$ and need not to be considered in the q range applied in the present experiment. It is well-known that ellipsoids of revolution and polydisperse spheres give rise to the same scattering curves; in fact this relation is explicitly used in the analysis of the scattering data. Dynamic LS measurements which will be discussed in detail in a forthcoming contribution[9] show that the polydispersity of the micelles is in the range of anionicaly polymerized polystyrene standard samples. From cumulant fitting to the time autocorrelation function we obtained a relative width of the distribution $w \cong 0.02$ for a polystyrene sample with a polydispersity $M_W/M_n = 1.02$. For micellar solutions of the samples described here the corresponding value was found to be $w < 0.03$. Thus, the assumption that the micelles are almost monodisperse ellipsoids of revolution rather than polydisperse spheres appears to be quite reasonable.

As was pointed out by Hosemann,[22] an ellipsoid in a distinct spatial orientation gives rise to the same scattering intensity at given q as the sphere inscribed between the tangents to the ellipsoid which are perpendicular to the direction of incidence. With α being the angle between the direction of incidence and the minor semiaxis of the ellipsoid, the respective radius of that sphere is given by $R(A,\epsilon,\alpha) = A(\sin^2\alpha + \epsilon^2\cos^2\alpha)^{1/2}$, where A is the major semiaxis of the ellipsoid and ϵ is the ellipticity, i.e., the ratio of minor and major semi-axis. Integration over all possible orientations of the ellipsoid with respect to the incident beam leads to the scattering intensity of an ellipsoid of revolution.

The particle scattering factor of an ellipsoid of revolution consisting of a core and a shell may thus be written as[8]

$$P(q, A,\epsilon) = \int_0^{\pi/2}\Big[\frac{1}{M}[\Delta\sigma_s V(A_s,\epsilon_s)F(q,R(A_s,\epsilon_s,\alpha)) + (\Delta\sigma_c - \Delta\sigma_s)V(A_c,\epsilon_c)F(q,R_c(A_c,\epsilon_c,\alpha))]\Big]^2 \cos\alpha\, d\alpha \quad (1a)$$

Here A_s and A_c are the major semiaxes of the shell and the core, respectively, and ϵ_s and ϵ_c are the corresponding ellipticities which may have different values. $\Delta\sigma_s$ and $\Delta\sigma_c$ are the excess SLDs of the shell and core defined as $\Delta\sigma = \sigma - \sigma_0$, where σ_0 represents the SLD of the solvent. $F(q,R)$ is the well-known particle scattering factor of a homogeneous sphere with radius R.[23] M is given by $M = \Delta\sigma_s V(A_s,\epsilon_s) + (\Delta\sigma_s - \Delta\sigma_c)V(A_c,\epsilon_c)$, where $V = 4\pi\epsilon A^3/3$ is the volume of the respective ellipsoid. Equation 1a can be easily generalized to a multishell model with $j = 2, 3, 4, \ldots n$, where the innermost shell with $j = n$ is what we previously have called the core. The particle scattering factor is than given as

$$P(q, A,\epsilon) = \int_0^{\pi/2}\Big[\frac{1}{M}[\Delta\sigma_1 V(A_1,\epsilon_1)F(q,R(A_1,\epsilon_1,\alpha) + \sum_{j=2}^{n}(\Delta\sigma_j - \Delta\sigma_{j-1})V(A_j,\epsilon_j)F(q,R(A_j,\epsilon_j,\alpha))]\Big]^2 \cos\alpha\, d\alpha \quad (1b)$$

The incorporation of butanol in the micelle causes a change of the excess SLD of the incorporation site and thereby changes the scattering function. This would be seen most prominently if only the incorporated alcohol would contribute to the excess scattering, a situation which may be experimentally approached, if first the solvent SLD is matched to the mean SLD of the micelle containing protonated butanol, which reduces the mean excess SLD to zero ($\Delta\sigma_c \approx 0$, $\Delta\sigma_s \approx 0$) and then the protonated alcohol is substituted by the deuterated species which enhances the SLD of the incorporation site. Let us now consider two possible limiting cases for the distribution of the butanol in the micelles. If the deuterated alcohol was solubilized exclusively into the hydrophobic core of the micelle, the contrast of the core would be enhanced ($\Delta\sigma_c > 0$) whereas the outer shell still remains invisible ($\Delta\sigma_s \approx 0$). In this case the neutrons would see a homogeneous ellipsoid of revolution of a size corresponding to that of the core of the micelle and the particle scattering factor given by eq 1a is reduced to

$$P(q, A,\epsilon) = \int_0^{\pi/2} F^2(q,R(A_c,\epsilon_c,\alpha)) \cos\alpha\, d\alpha \quad (2)$$

Alternatively, if the alcohol is exclusively incorporated into the amphiphile film such that the alcohol molecules build a corona at the edge of the hydrophobic core, the contrast of the shell is enhanced ($\Delta\sigma_s > 0$) while the core remains invisible ($\Delta\sigma_c \approx 0$). In this case eq 1a reduces to

$$P(q, A,\epsilon) = \int_0^{\pi/2}\left[\frac{V(A_s,\epsilon_s)F(q,R(A_s,\epsilon_s,\alpha)) - V(A_c,\epsilon_c)F(q,R_c(A_c,\epsilon_c,\alpha))}{V(A_s,\epsilon_s) - V(A_c,\epsilon_c)}\right]^2 \cos\alpha\, d\alpha \quad (3)$$

Note that both eqs 2 and 3 do no longer involve the excess scattering length density $\Delta\sigma$ as a variable. In Figure 4 scattering data corrected for solvent and background scattering from the samples with deuterated butanol are shown together with the best fits by $I(q) = NP(q, A,\epsilon)$, where N is a normalization constant and $P(q, A,\epsilon)$ is the particle scattering factor according to either eq 2 or 3. With the particle scattering factor of an homogeneous ellipsoid of revolution according to eq 2 (upper part of Figure 4) it is not possible to obtain satisfactory fits to the experimental data. While the inner parts of the scattering curves up to $q = 1.6-2.0$ nm^{-1} are reasonably well approximated, the model fails completely to describe the outer parts of the scattering curves. On the other hand, the model for the preferential incorporation of the alcohol into the amphiphile film represented by eq 3 (lower part of Figure 4) gives excellent results. The scattering curves are well approximated over the whole experimental q range. The parameters from the best fits by eq 3 are collected in Table 1.

Due to the shelled structure of the C_nG_m micelles, it is only possible to match the mean SLD of the micelles by variation of the solvent SLD while the SLDs of the individual shells cannot be matched. We therefore attempted to further refine the description of the experimental data with the particle scattering factor of a triple-shell ellipsoid of revolution according to eq 1b, allowing all three shells to have nonzero excess SLDs. The SLD σ_j of the jth shell was calculated from the SLDs of the single components using

$$\sigma_j = \sum_i \Phi_i \sigma_i \quad (4)$$

with Φ_i denoting the partial molar volume fraction which was approximated by the molar volume fraction of component i and σ_i the SLD of the pure component. For the estimation of the SLD of the H_2O/D_2O mixture with $X_H = 0.9$, the solubilized amount of butanol in the intermicellar solution should be taken into account. The SLD of the H_2O/D_2O mixture with $X_H = 0.9$ without butanol is calculated by using eq 4 as $\sigma_0 = 0.13 \times 10^{10}$ cm^{-2}. From preliminary headspace gas chromatographic measurements[24-26] on the partition of butanol in micellar solutions of C_nG_m we know that 80% of the total amount of the butanol are in the intermicellar solution and 20% are

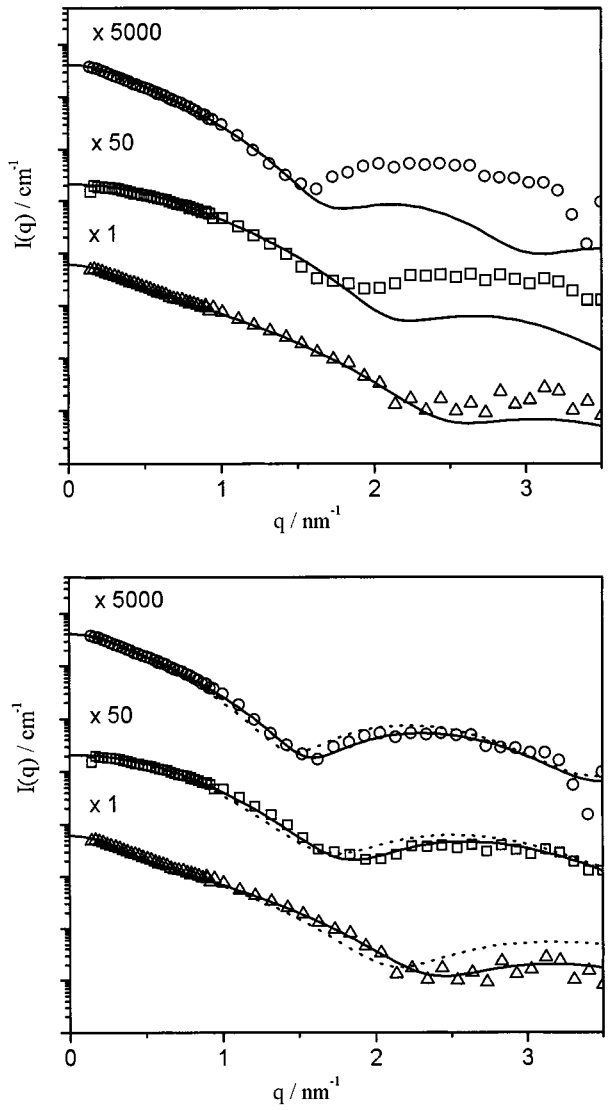

Figure 4. Scattered intensity versus scattering vector from β-C_8G_1-DB (△), β-$C_{10}G_2$DB (□), and β-$C_{12}G_2$DB (○) solutions. The symbols are experimental data in units of water scattering, corrected for solvent and background scattering. The full lines are model fits according to eq 2 (upper) and eq 3 (lower). The dotted lines in the lower part are model calculations according to eq 1b, for details see text. For clarity the curves are shifted by factors as indicated in the figure.

TABLE 1: Major Semiaxes of the Core A_c and the Shell A_s and the Corresponding Ellipticities ϵ_c and ϵ_s of the Prolate Ellipsoidal Micelles Investigated[a]

	A_s/ nm	A_c/ nm	ϵ_s	ϵ_c	d_A/ nm	d_ϵ/ nm	l_c/ nm	$\langle A\rangle$/ nm	N
β-C_8G_1	1.45	0.90	6.0	9.0	0.55	0.60	1.17	1.18	0.6162
β-$C_{10}G_2$	1.75	1.26	2.1	2.5	0.49	0.53	1.42	1.51	0.4283
β-$C_{12}G_2$	1.95	1.42	3.8	4.9	0.53	0.45	1.68	1.69	0.8260

[a] The values were obtained by a nonlinear least-squares fit of eq 3 to the experimental data. The parameters d_A and d_ϵ are the thickness of the shell in the direction of the major and minor semi-axis respectively, l_c is the extended chain length of the surfactant alkyl chain according to Tanford,[30] and $\langle A\rangle$ is the average length of the major semiaxis. In the last column the normalization constant N is listed.

incorporated into the micelles, thus leading to a molar alcohol/surfactant ratio of about 1 in the micelles of all three surfactants and to a molar alcohol/solvent ratio of 0.01 in the intermicellar solution. Taking into account the deuterated butanol which is molecularly dispersed ($\sigma = 6.64 \times 10^{10}$ cm^{-2}), the SLD of the solvent may thus be estimated to $\sigma_0 = 0.39 \times 10^{10}$ cm^{-2}. The

TABLE 2: Parameters Used for the Calculations of the Scattering Factor of a Triple Shell Ellipsoid According to Eq 1b (Dotted Line in Figure 4)[a]

	A_1/nm	ϵ_1	$\Delta\sigma_1$/ 10^{10} cm^{-2}	$\Delta\sigma_2$/ 10^{10} cm^{-2}	$\Delta\sigma_3$/ 10^{10} m^{-2}
β-C_8G_1	1.62	5.6	0.39	6.25	−0.77
β-$C_{10}G_2$	1.98	2.2	0.37	6.25	−0.76
β-$C_{12}G_2$	2.35	3.45	0.37	6.25	−0.75

[a] The axes and ellipticities were taken from refs 8 and 9, and the SLDs were calculated using the molar volumes of the headgroups according to Dupuy et al.[28] and Antonelli et al.[29]

outermost shell ($j = 1$) in the triple-shell model, which consists of the saccharide headgroups, contains according to Dupuy et al.[27,28] a number of solvent molecules per surfactant headgroup of about $n_{Sol} \sim 30$ in case of the maltosides $C_{10}G_2$ and $C_{12}G_2$. With a partial molar volume of the maltoside headgroup of $\upsilon_i = 0.341$ nm^3,[28] this leads to a value for the excess SLD of the outermost shell of $\Delta\sigma_1 = 0.37 \times 10^{10}$ cm^{-2}. To estimate the solvatization of the glucosidic headgroup, we assume that the number of solvent molecules per glucosidic unit per headgroup is constant which leads to $n_{Sol} \sim 15$ for the headgroup of the C_8G_1. From the thermodynamic data presented by Antonelli et al.,[29] one can estimate the partial molar volume of the glucosidic headgroup to be $\upsilon_i = 0.184$ nm^3. Accordingly, the excess SLD of the outermost shell is then $\Delta\sigma_1 = 0.39 \times 10^{10}$ cm^{-2} in the case of C_8G_1. The intermediate shell ($j = 2$) is built of the deuterated butanol and is located at the transition from hydrophilic headgroup region to hydrophobic core of the micelle. Since the mean SLD of the micelle is matched by the solvent SLD, the contribution from the surfactant molecules to the SLD of the second shell can be neglected and the excess SLD is calculated from the bulk value of deuterated butanol to be $\Delta\sigma_2 = 6.25 \times 10^{10}$ cm^{-2}. The innermost shell ($j = 3$) is the hydrocarbon core and the excess SLD is estimated to be about $\Delta\sigma_3 \approx -0.76 \times 10^{10}$ cm^{-2}. The geometrical parameters for the second and third shell are taken from Table 1 with $A_3 = A_c$, $A_2 = A_s$, and the ellipticities ϵ_3 and ϵ_2, respectively. For the outermost shell the parameters are known from additional SANS experiments.[8,9] The parameters are summarized in Table 2.

Introducing the parameters from Tables 1 and 2 into eq 1b yields the dotted lines in Figure 4b, which describe the experimental data not as convincingly as the fits by eq 3. Actually, if eq 1b is used to fit the experimental data with all parameters floating freely, the results from Table 1 are reproduced and both $\Delta\sigma_1$ and $\Delta\sigma_3$ are found to be insignificantly different from zero. We are therefore confident that the parameters listed in Table 1 describe the shape and size of the micelles correctly. These parameters together with the findings in our other works[8,9] translate into a model for the mixed butanol/β-C_nG_m micelles under investigation as sketched in Figure 5. Although this sketch may be oversimplifying to a certain extent, we will use it to discuss the numbers in Table 1 in more detail. According to the above discussion only the shell containing the deuterated butanol causes the observed excess scattering, whereas the outer shell and the core remain invisible. The thickness of this shell $d = A_s - A_c \approx \epsilon_s A_s - \epsilon_c A_c$ should therefore be equal in all three cases and it should correspond to the size of a butanol molecule. In Table 1 the values for $d_A = A_s - A_c$ and for $d_\epsilon = \epsilon_s A_s - \epsilon_c A_c$ are listed. According to Tanford,[30] the all-trans chain length l_c of alkyl chains is estimated as

$$l_c/\text{nm} = 0.127n + 0.154 \qquad (5)$$

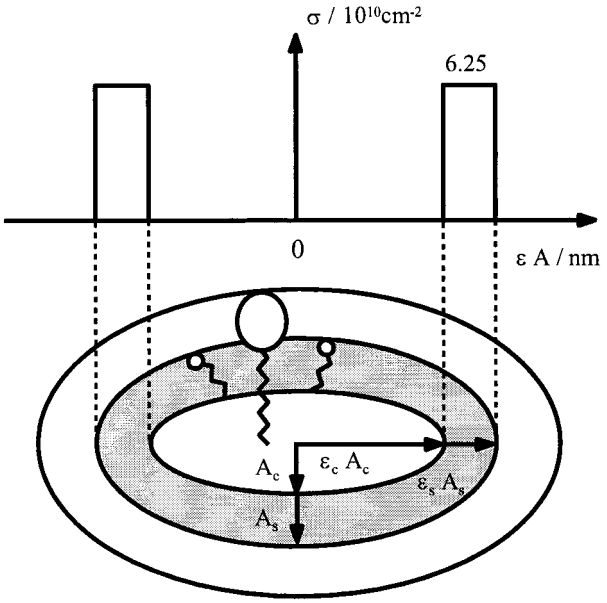

Figure 5. Sketch of a compound C_nG_m/butanol micelle. In the contrast matching experiment the solvent was selected such that the surfactant is quasi invisible. The resulting shell consisting of deuterated butanol causes the observed excess scattering.

where n is the number of carbon atoms. This yields $l_c \approx 0.65$ nm for the butyl chain. The thickness of the butanol shell is calculated from Table 1 as $d = (0.53 \pm 0.05)$ nm, i.e., $d \cong 0.8l_c$(butanol).

Further, one might expect the average length of the major semiaxes $\langle A \rangle = (A_c + A_s)/2$ to be related to the chain length of the hydrocarbon moiety of the respective surfactant. Indeed we find very good agreement if we compare the average values, calculated from the first and second column in Table 1 with the all-trans chain length of the hydrocarbon moiety of the surfactant. These agreements show that the suggested model for the structure of the compound micelles, i.e., assemblies of prolate ellipsoidal shape with butanol preferentially located at the hydrophilic hydrophobic interface, is thoroughly consistent. This result is well in line with the previous finding that compound β-C_8G_1/butanol micelles grow with respect to the rotational axis upon the addition of moderate amounts of butanol, while the cross-sectional radius of the micelle remains almost unchanged.[8] A solubilization of the alcohol into the hydrophobic core should result in a swelling of the micelles and would not necessarily change the overall shape significantly. If, in contrast, the alcohol acts as a cosurfactant, as we observed here, the mean effective area per hydrophilic headgroup decreases with the number of alcohol molecules incorporated into the micelle. Consequently, the natural curvature of the hydrophilic hydrophobic interface is reduced in the same direction, which accounts for the observed elongation of the compound β-C_8G_1/butanol micelles with increasing amount of butanol.

As was stated before, the model may be oversimplifying, especially by presuming a homogeneous distribution of the butanol in the mixed micelles. It has been shown by several authors that in mixed micelles components with large headgroup and small volume of the hydrophobic chain are enriched in the parts with greater curvature of the amphiphilic film.[31−35] In the present case, this could mean that the butanol is more likely to be found in the flat "middle" part of the ellipsoid than in the highly curved "endings". Consequently, the SLD of the butanol shell formed at the hydrophobic/hydrophilic interface would not be homogeneous, but higher in the "middle" and lower at the "endings" due to different values of the butanol volume fraction. This is qualitatively well in line with the finding that the thickness of the shell consisting of butanol is only about 80% of the extended butanol chain length. However, it is not possible to conclude on this segregation effect quantitatively from SANS data from isotropic solutions, as was shown by Hendrikx et al.[36] The question has to be spared for experiments on lyotropic nematic phases.

Conclusions

The mean scattering length density of compound micelles of alkyl mono- and diglucosides with butanol was matched by a H_2O/D_2O mixture with a mole fraction of light water $X_H = 0.9$. After the protonated alcohol is substituted with deuterated butanol, the neutron small-angle scattering data can be described with the theoretical form factor for a hollow ellipsoidal shell with a shell thickness corresponding to the length of a butanol molecule. This leads us to conclude that the butanol acts as a cosurfactant which is enriched at the interface separating the hydrophobic from the hydrophilic part of the micelles. In combination with earlier results on β-C_8G_1 solutions[8] and recent studies on β-alkylmaltosides,[9] we are led to the presumption that butanol induces the formation of anisotropic C_nG_m micelles by reducing the effective area per headgroup. One may speculate that this enhances the tendency of C_nG_m surfactants to the formation of lyotropic mesophases such that in the ternary mixtures the liquid crystalline phases occur at much lower surfactant content as compared to the binary mixtures.

Acknowledgment. We thank the Berlin Neutron Scattering Center (BENSC) at the HMI for beamtime and technical support. This work was supported by the Deutsche Forschungsgesellschaft which is gratefully acknowledged.

References and Notes

(1) Miller, C.A.; Gradzielski, M.; Hoffmann, H.; Krämer, U.; Thunig, C. *Prog. Colloid Polym. Sci.* **1991**, *84*, 243.
(2) Platz, G.; Thunig, C.; Hoffmann, H. *Ber. Bunsenges. Phys. Chem.* **1992**, *96*, 667.
(3) Gazeau, D.; Bellocq, A. M.; Roux, D.; Zemb, T. *Europhys. Lett.* **1989**, *9*, 447.
(4) Balinov, B.; Olsson, U.; Söderman, O. *J. Phys. Chem.* **1991**, *95*, 5931.
(5) Hoffmann, H.; Thunig, C.; Munkert, U. *Langmuir* **1992**, *8*, 2629.
(6) Platz, G.; Thunig, C.; Pölike, J.; Kirchhoff, W.; Nickel, D. *Colloids Surf. A* **1994**, *88*, 113.
(7) Mitchell, T. J.; Tiddy, G. J. T.; Warring, L.; Bostock, T.; McDonald, M. P. *J. Chem. Soc., Faraday Trans. 1* **1983**, *79*, 358.
(8) Möller, A.; Lang, P.; Findenegg, G. H.; Keiderling, U. *Ber. Bunsenges. Phys. Chem.* **1997,** *101*, 1121.
(9) Möller, A.; Lang, P.; Findenegg, R. H.; Keiderling, U. Manuscript in preparation.
(10) Jagannathan, N.; Venkateswaran, K.; Herring, F.; Patey, G.; Walker, D. *J. Phys. Chem.* **1987**, *91*, 4553.
(11) Szajdzinska-Pietek, E.; Maldonado, R.; Kevan, L.; Jones, R. *J. Colloid Interface Sci.* **1986**, *110*, 514.
(12) Baglioni, P.; Kevan, L. *J. Phys. Chem.* **1987,** *91*, 2106.
(13) Dvolaitzky, M.; Taupin, C. *Nouv. J. Chim.* **1977**, *1*, 355.
(14) Hayter, B.; Hayoun, M.; Zemb, T. *Colloid Polym. Sci.* **1984**, 262, 798.
(15) Mukerjee, P. *Solution Chemistry of Surfactants, Vol. 1*; Plenum: New York, 1979; p 153; *Pure Appl. Chem.* **1980**, *52*, 1317.
(16) Keiderling, U.; Wiedenmann, A. *Physica B* **1995**, *213&214*, 895.
(17) Keiderling, U. *Physica B* **1997**, *234−236*, 1111.
(18) Glatter, O. *Acta Phys. Austriaca* **1977**, *47*, 83. Glatter, O. *J. Appl. Crystallogr.* **1977**, *10*, 415.
(19) Müller, K.; Glatter, O. *Makromol. Chem. 183*, **1982**, 465.
(20) Lindner, P.; Zemb, Th. *Neutron, X-Ray and Light Scattering: Introduction to an investigative tool for colloidal and polymeric systems*; North-Holland: Amsterdam, Oxford, New York, Tokyo, 1991; p 109.
(21) For an overview, see Glatter, O.; Kratky, O. *Small-Angle X-ray Scattering*; Academic Press: London, 1982.

(22) Hosemann, R. *Z. Phys.* **1939**, *113*, 751.

(23) Rayleigh, Lord *Proc. R. Soc. London, Ser A* **1911**, *84*, 25.

(24) Spink, C. H.; Colgan, S. *J. Phys. Chem.* **1983**, *87*, 888.

(25) Morgan, M. E.; Uchiyama, H.; Christian, S. D.; Tucker, E. E.; Scamehorn, J. F. *Langmuir* **1994**, *10*, 2170.

(26) Wan-Badhi, W.; Bloor, D. M.; Wyn-Jones, E. *Langmuir* **1994**, *10*, 2219.

(27) Dupuy, C.; Auvray, X.; Petipas, C.; Anthore, R.; Costes, F.; Rico-Lattes, I.; Lattes, A. *Langmuir* **1996**, *12*, 3162.

(28) Dupuy, C.; Auvray, X.; Petipas, C.; Rico-Lattes, I.; Lattes, A. *Langmuir* **1997**, *13*, 3965.

(29) Antonelli, M. L.; Bonicelli, M. G.; Ceccaroni, G.; La Mesa, C.; Sesta, B. *J. Coll. Polym. Sci.* **1994**, *272*, 704.

(30) Tanford, C. *The hydrophobic effect*; Wiley: New York, 1973.

(31) Hendrikx, Y.; Charvolin, J.; Rawiso, M. *J. Colloid Interface Sci.* **1984**, *100*, 597.

(32) Alperine, S.; Hendrikx, Y.; Charvolin, J. *J. Phys. Lett.* **1985**, *46*, L27.

(33) Gelbart, W. M.; McMullen, W. E.; Masters, A.; Ben-Shaul, A. *Langmuir* **1985**, *1*, 101.

(34) Mather, D. E. *J. Colloid Interface Sci.* **1976**, *57*, 240.

(35) Lin, T.-L.; Liu, C.-C.; Roberts, M. F.; Chen, S.-H. *J. Phys. Chem.* **1991**, *95*, 6020.

(36) Hendrikx, Y.; Charvolin, J.; Rawiso, M.; Liebert, L.; Holmes, M. C. *J. Phys. Chem.* **1983**, *87*, 3991.